Supplementary Information

Feeding ten billion people is possible within four terrestrial planetary boundaries

Dieter Gerten, Vera Heck, Jonas Jägermeyr, Benjamin Leon Bodirsky, Ingo Fetzer, Mika Jalava, Matti Kummu, Wolfgang Lucht, Johan Rockström, Sibyll Schaphoff, Hans Joachim Schellnhuber

Supplementary Figures

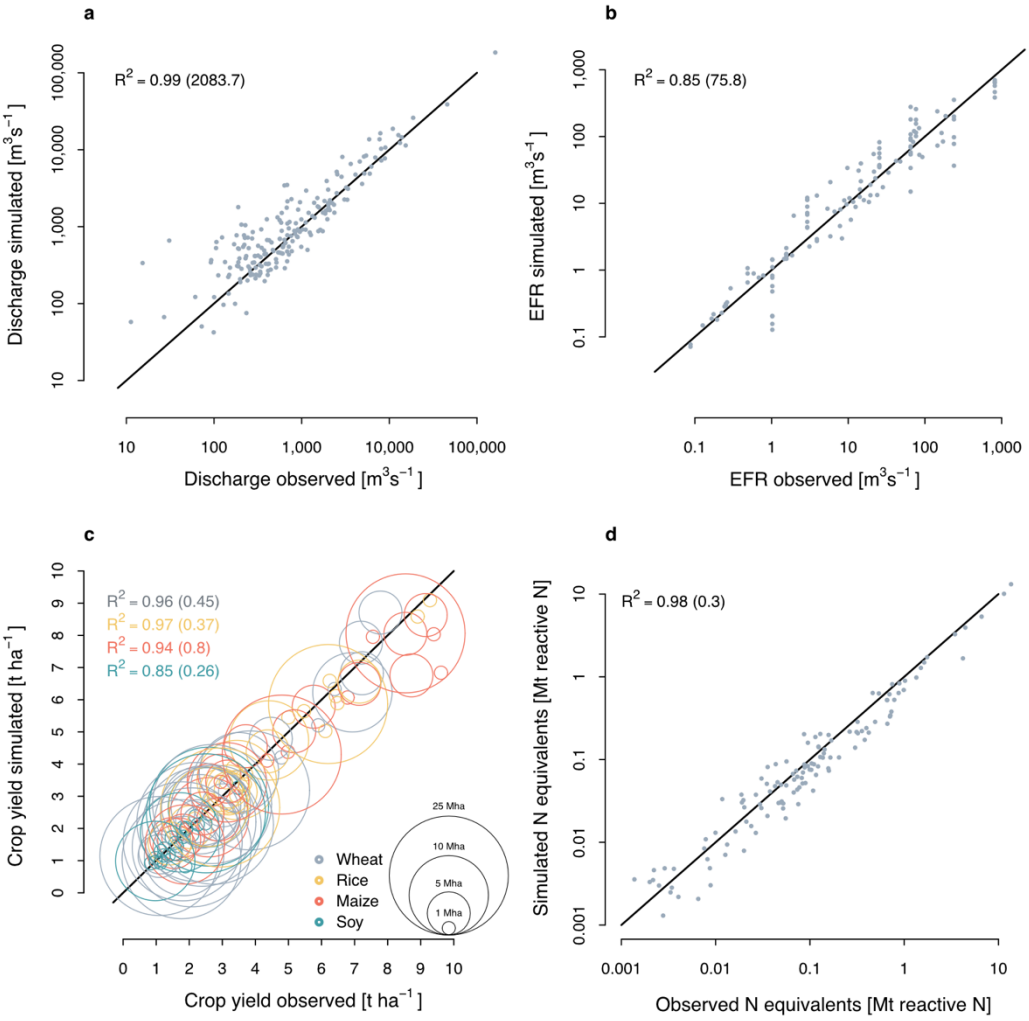

Supplementary Figure 1. Evaluation of LPJmL-simulated spatial patterns of river discharge, environmental flow requirements (EFRs), crop yields and nitrogen (N) harvest vs. observational data. Results are averaged over 1980–2009, representing uncalibrated mean annual discharge (m^3 s^{-1}) of ~200 river basins (**a**), EFRs (m^3 s^{-1}) for 132 basins (**b**), country-level crop yields, calibrated for management intensity, of main staple crops for the respective top 30 producer countries (t ha^{-1}), with chart symbols scaled by the country's cropland area (**c**), and country-level crop production in N equivalents in 2005 (log Mt reactive N). Also given are the coefficient of determination (R^2) and the root mean square error (in parentheses). Observed discharge[1] only includes gauges with >100 months of available records and a <15% mismatch between reported and simulated contributing area. EFR data are for a wide range of streamflow and climate regimes, incorporating case studies with 10–50 years of daily flow observations and various EFR estimation methods (details in Methods and ref.[2]). Crop yields are evaluated against ref.[3], N data against ref.[4].

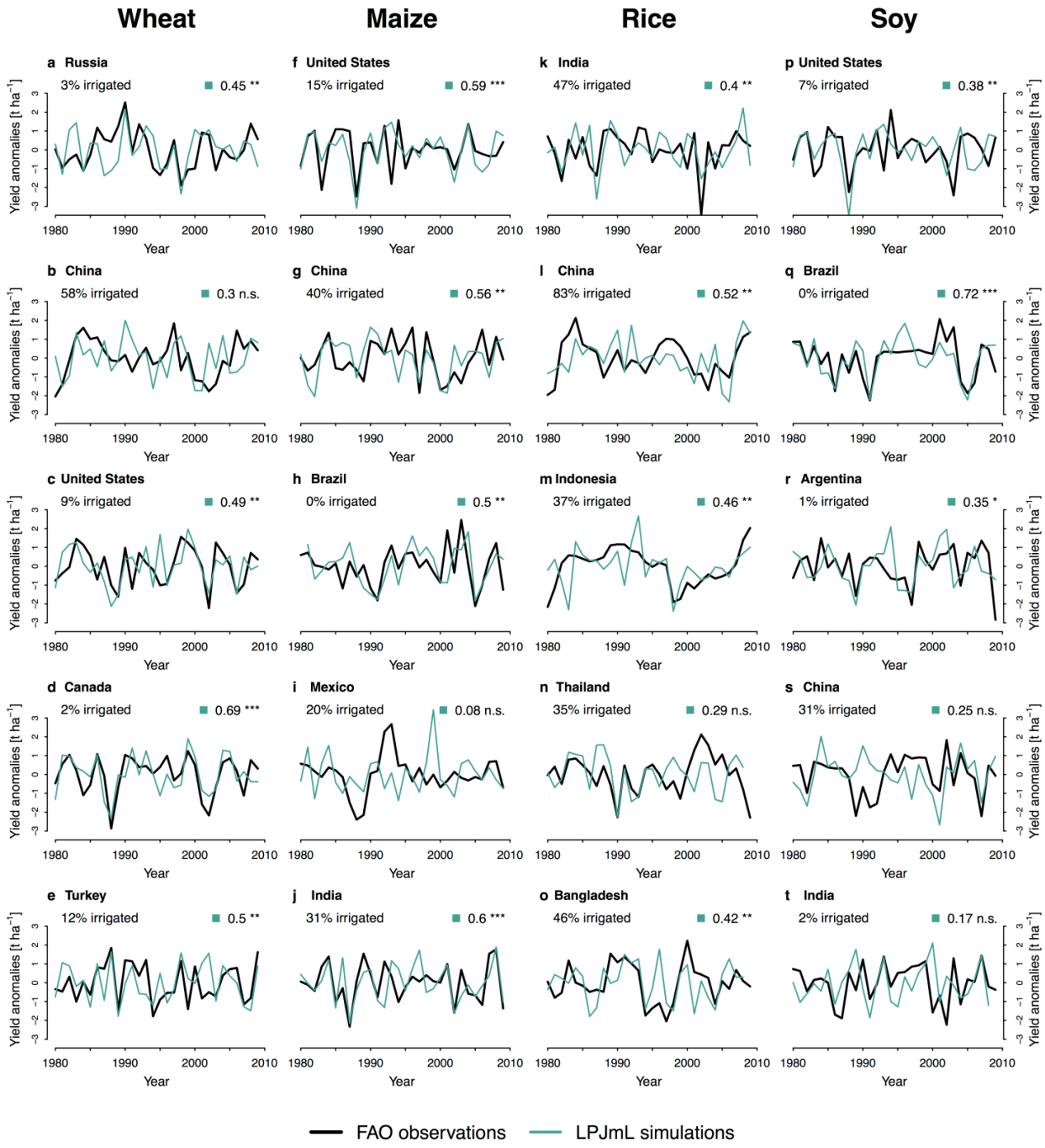

Supplementary Figure 2. Evaluation of LPJmL-simulated crop yield variability *vs.* observations. Country-level time series of de-trended yield anomalies from FAOSTAT[3] and LPJmL simulations for major crop types and their top five producing countries. Pearson's correlation coefficient is indicated in the top right corner of each plot (***, p <0.001; **, p <0.05; *, p <0.1; n.s., not significant); the fraction of cropland under irrigation is also indicated.

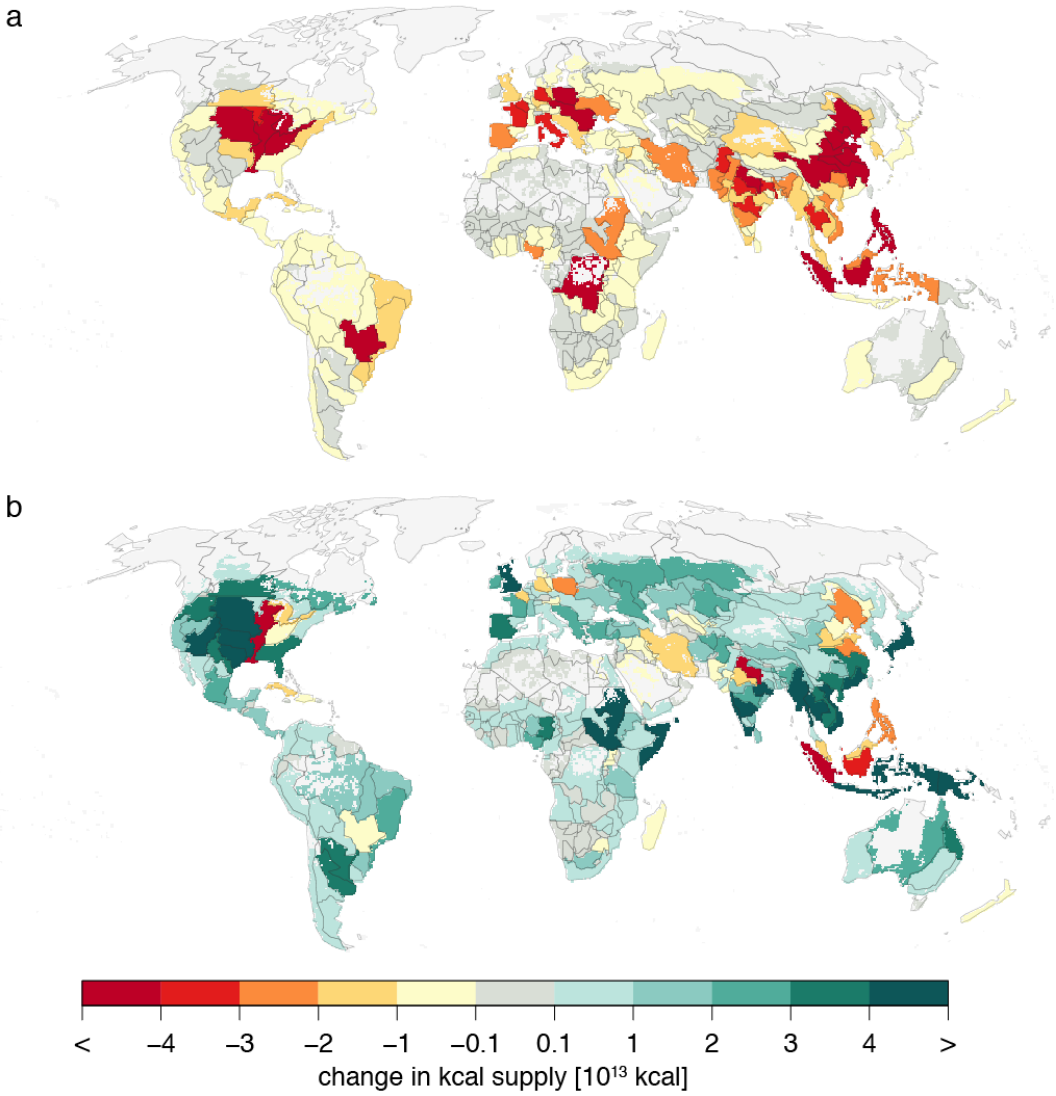

Supplementary Figure 3. Simulated absolute changes in net food supply (10^{13} kcal) per Food Producing Unit relative to year 2005. Changes through restoring the safe space, i.e. simultaneously respecting the planetary boundaries for biosphere integrity, land-system change, freshwater use, and N flows (**a**). Same, but assuming implementation of all considered management and socio-cultural opportunities within the safe space (**b**).

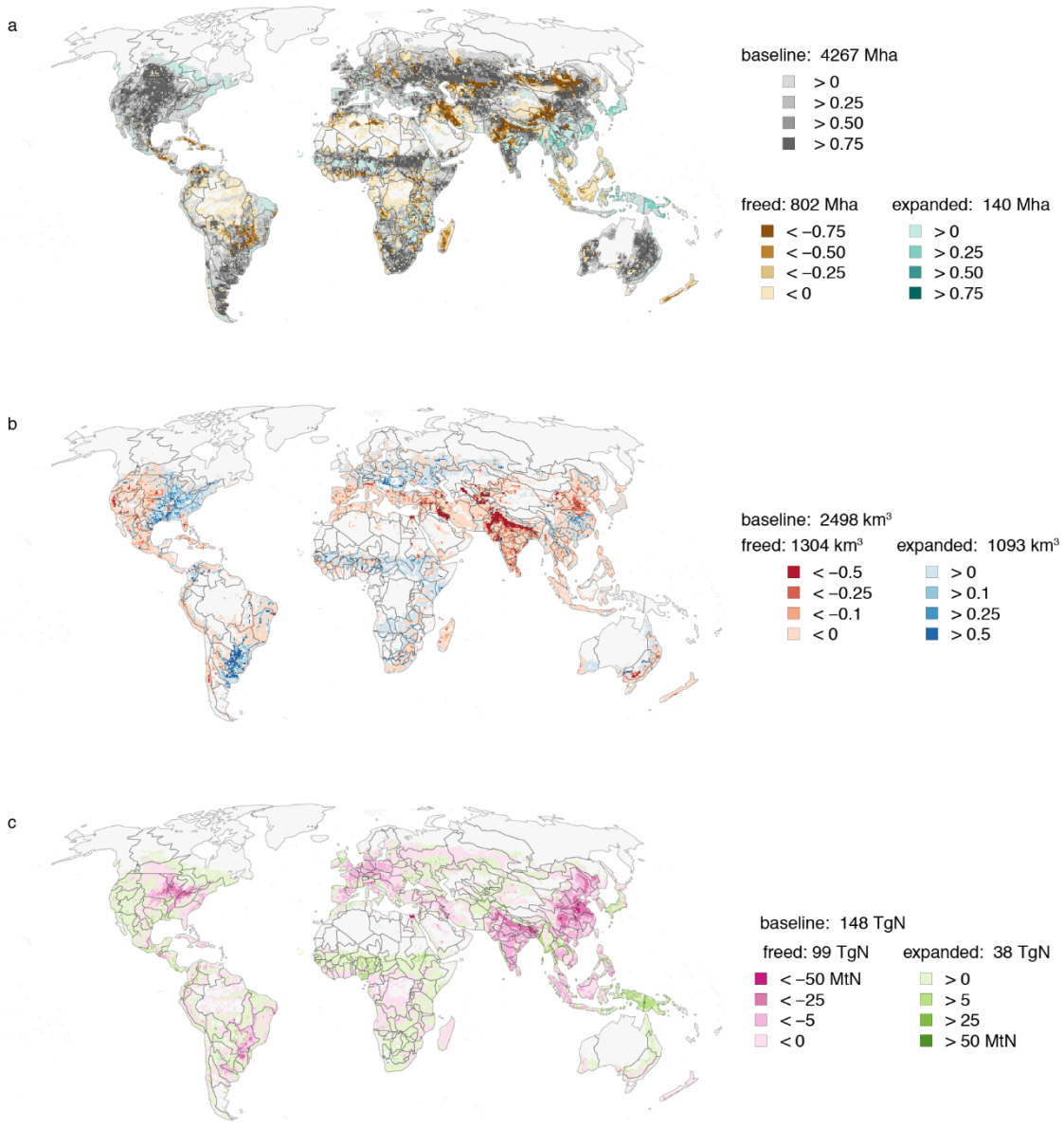

Supplementary Figure 4. Agronomic restrictions and opportunities within the planetary boundaries. Shown are effects on agricultural area, irrigation water use and nitrogen fertilization through restoration of the safe operating space and, respectively, through expansions within it. Fractional coverage with cropland and pastures in the reference period (grey), fractions freed (abandoned) for maintaining the boundaries for biosphere integrity and land-system change (brown), and fractions added through sustainable agricultural land expansion including restoration of degraded land (turquoise) (**a**). Change in water withdrawal (km^3 yr^{-1}) through either restriction (red) or expansion of irrigation (blue) within the safe space for freshwater use (**b**). Change in N fertilization (Mt) through either restriction (purple) or expansion (green) within the safe space for N flows (**c**). All data shown at 0.5° grid cell level and for 1980–2009.

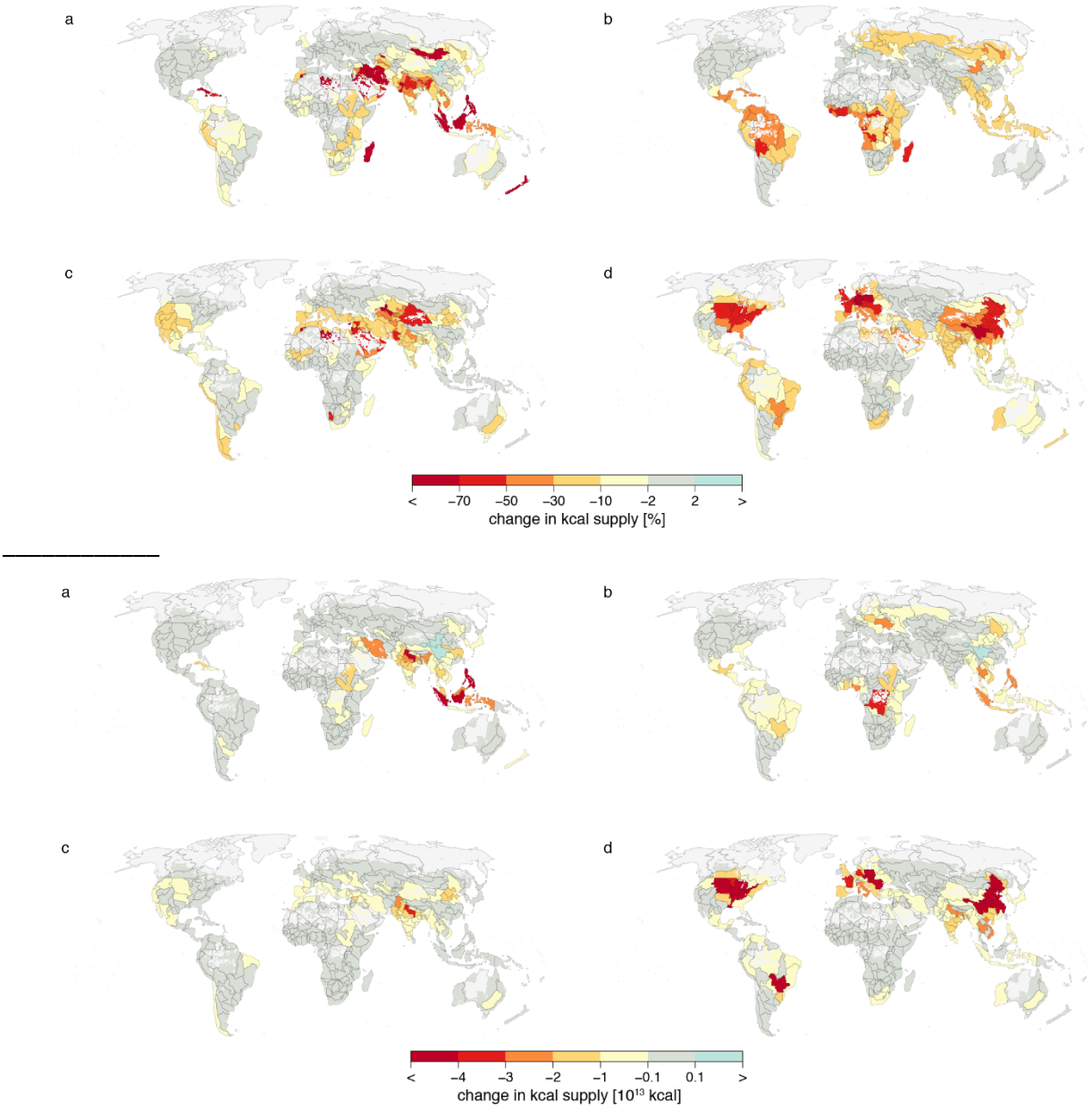

Supplementary Figure 5. Isolated food supply constraints when respecting the different planetary boundaries. Shown is the kcal net supply change (top panel, in percentage terms; bottom panel, in absolute terms) per Food Producing Unit relative to year 2005 conditions assuming that each individual boundary is respected in isolation: biosphere integrity (**a**), land-system change (b), freshwater use (**c**), N flows (**d**). Effects are not always additive as they represent the maximum effect not possibly cancelled out by respecting the boundaries considered in preceding calculation steps.

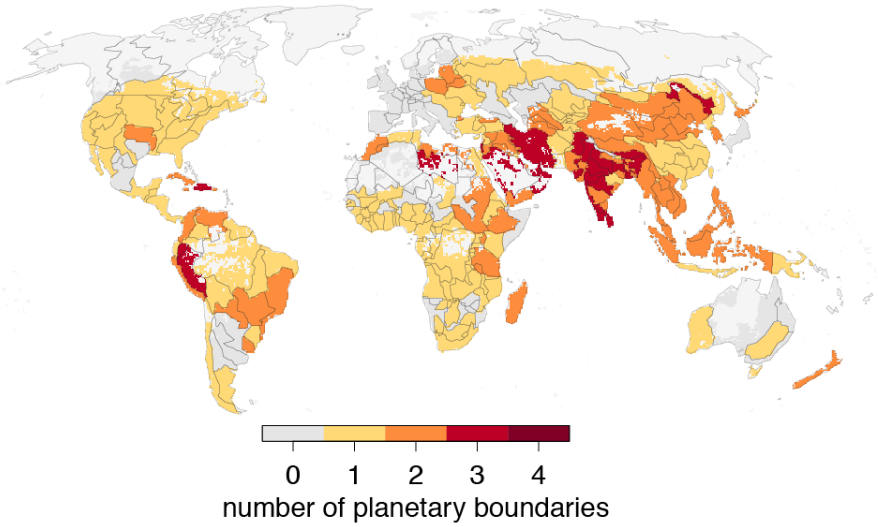

Supplementary Figure 6. Number of concurrently transgressed boundaries. Shown are only cases where >10% kcal net supply relies on transgression of the respective boundary. Dark grey areas: non-zero effects <10%; light grey areas: no effect.

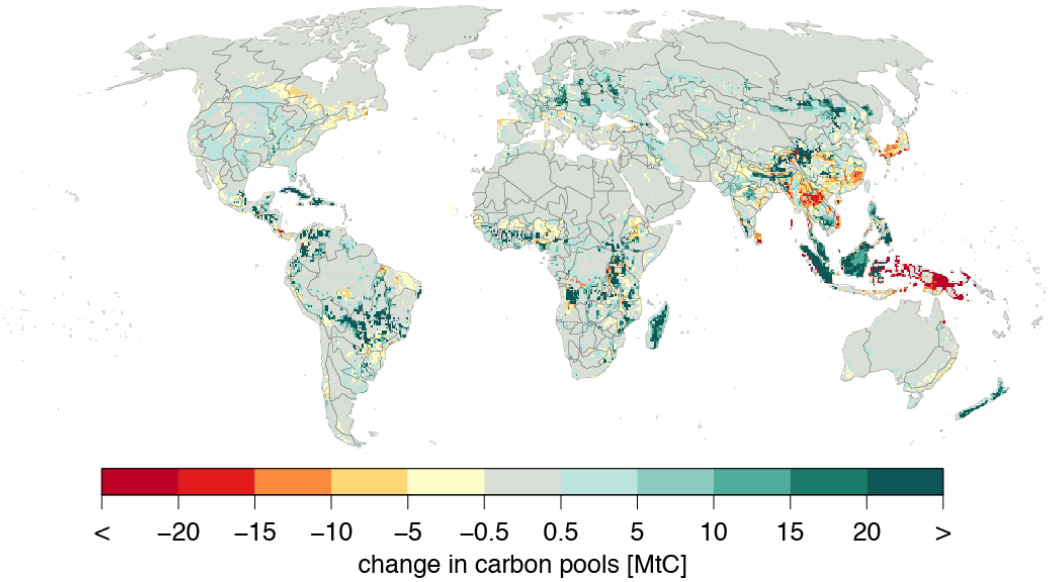

Supplementary Figure 7. Simulated change in carbon pools given implementation of all opportunities within the boundaries. Shown is the change in the total pool (sum of vegetation, litter and soil pools; MtC per grid cell) in an equilibrium run considering all opportunities compared to an equilibrium baseline run (*cf.* Suppl. Methods). Positive values (in green) indicate net C sequestration; decreases mainly occur in regions where agricultural expansion is still possible (*cf.* Suppl. Fig. 4).

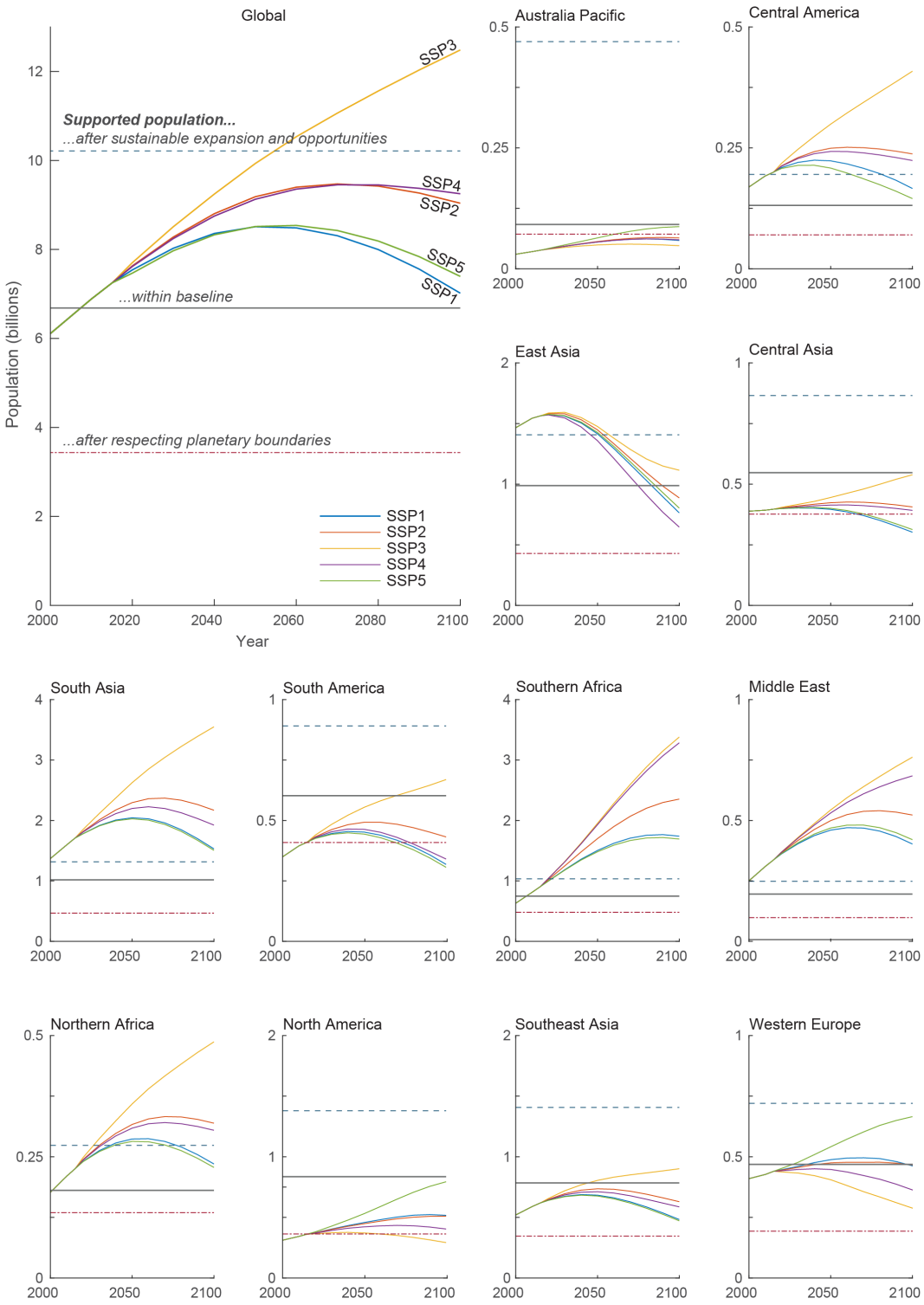

Supplementary Figure 8. Achievable food supply *vs.* projected populations in world regions. Time series of historical and projected future population (up to year 2100) globally (as in Fig. 2) and in world regions, for the different Shared Socio-Economic Pathways, as benchmarks for the net food supply in reference year 2005 (solid horizontal lines), when respecting all boundaries (lower dotted lines) and when implementing all opportunities (upper dashed lines), respectively.

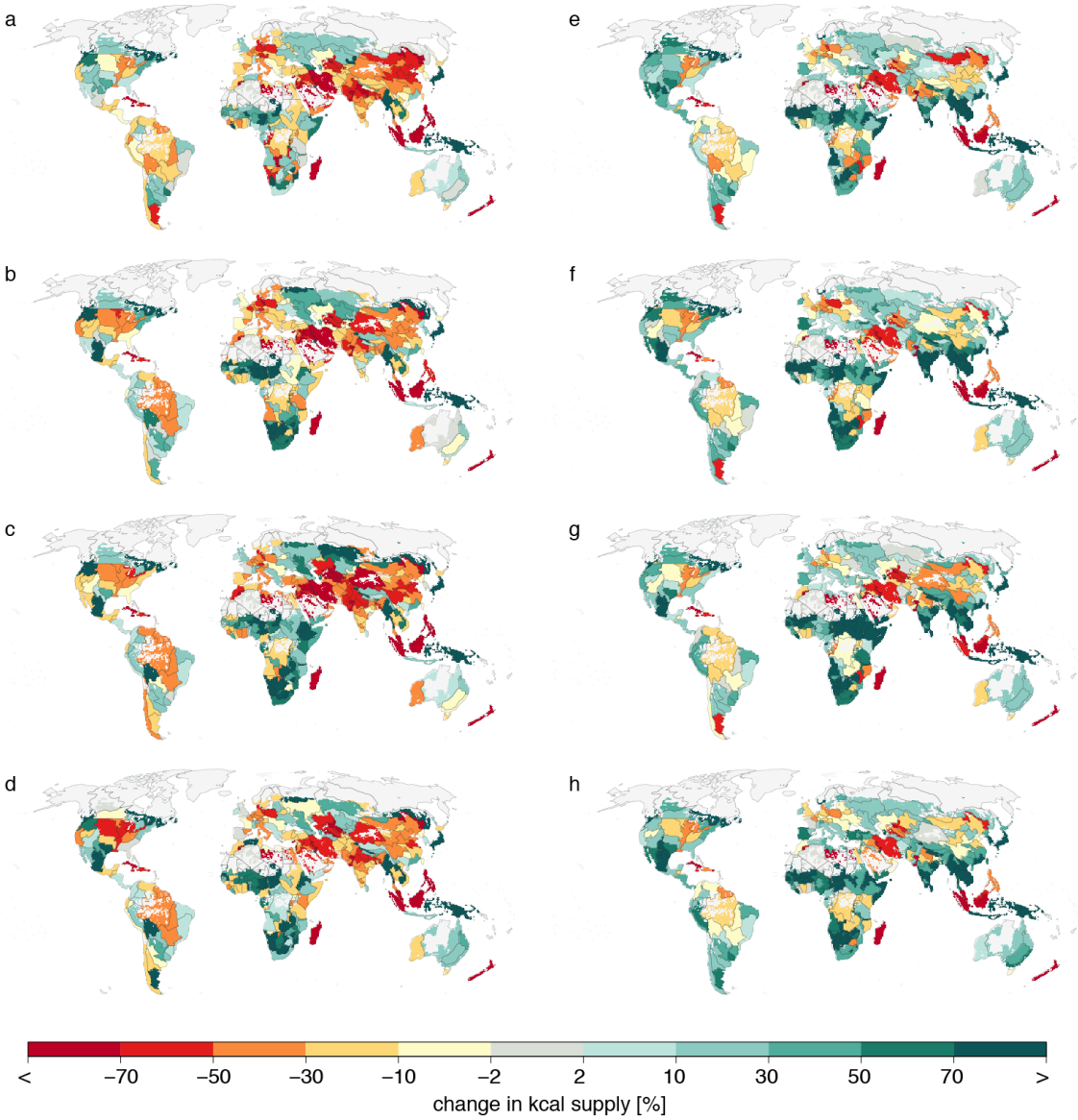

Supplementary Figure 9. Change in kcal net supply through sustainable intensification, but accounting for climate change impacts. Shown is the simulated change (%, FPU average) through irrigation, fertilizer and cropland expansion alone (left) and additionally with improved water/nutrient/land management (right) – for the same land-use pattern as in Fig. 3e,f but considering climate change impacts on underlying yields. **b–d** and, respectively, **f–h** show the changes simulated with bias-corrected output from three different General Circulation Models (HadGEM2-ES, IPSL-CM5A-LR, MIROC5) for the period 2030–2059 under an RCP2.6 emissions trajectory. The corresponding baseline from Fig. 3e,f is also shown for comparison (**a, e**). The resulting number of people that can be fed is 5.6–5.7 bn without the management options (baseline *cf.* Fig. 1: 5.4 bn) and 8.0–8.3 bn with them (baseline: 7.8 bn). The differences reflect complex impacts of climate change on yields and management, e.g. altered irrigation and fertilizer possibilities as well as higher plant water-use efficiency and biomass production due to rising atmospheric CO_2 content[5].

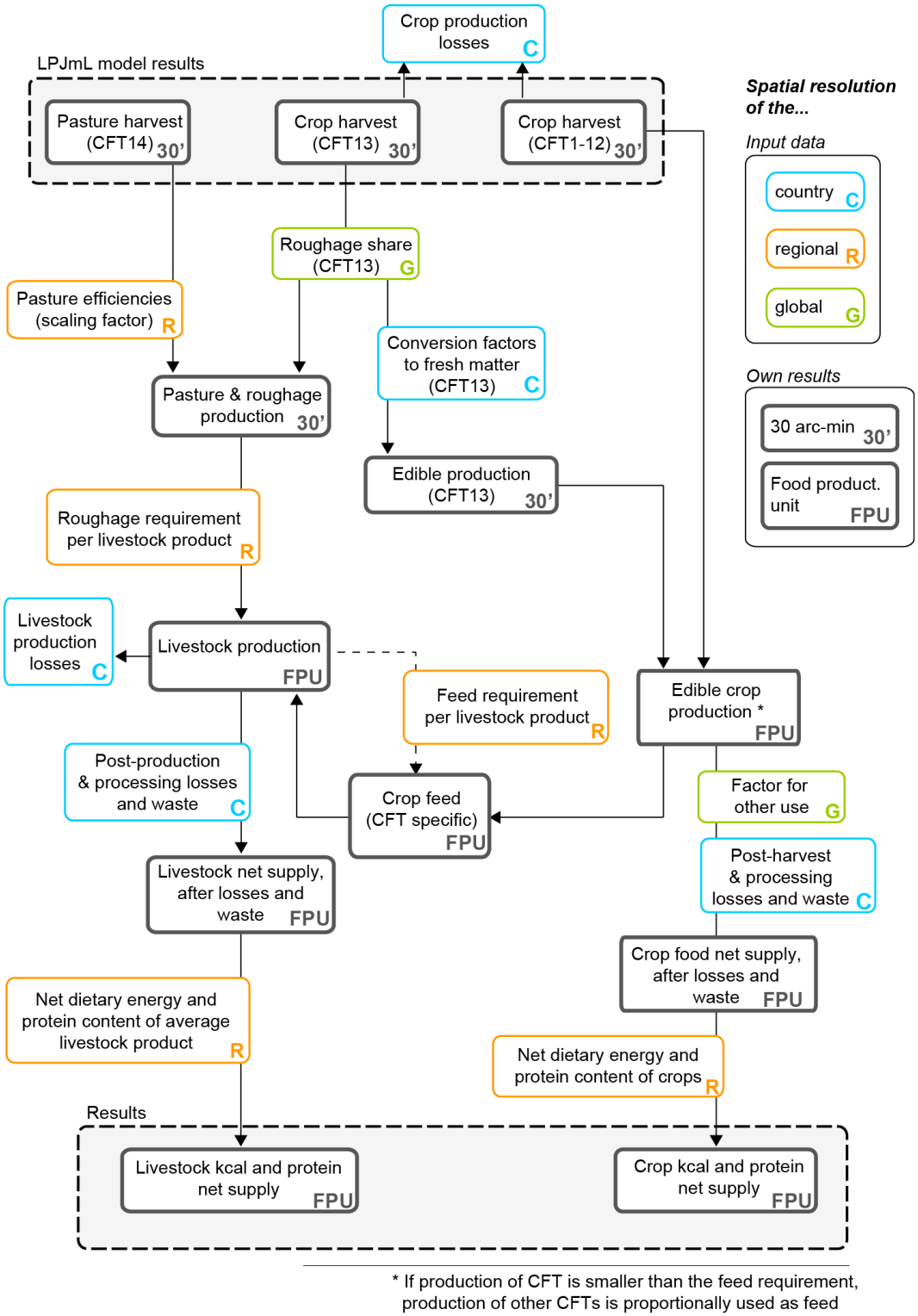

Supplementary Figure 10. Calculation scheme for livestock sector and diet scenarios. See Suppl. Methods for description.

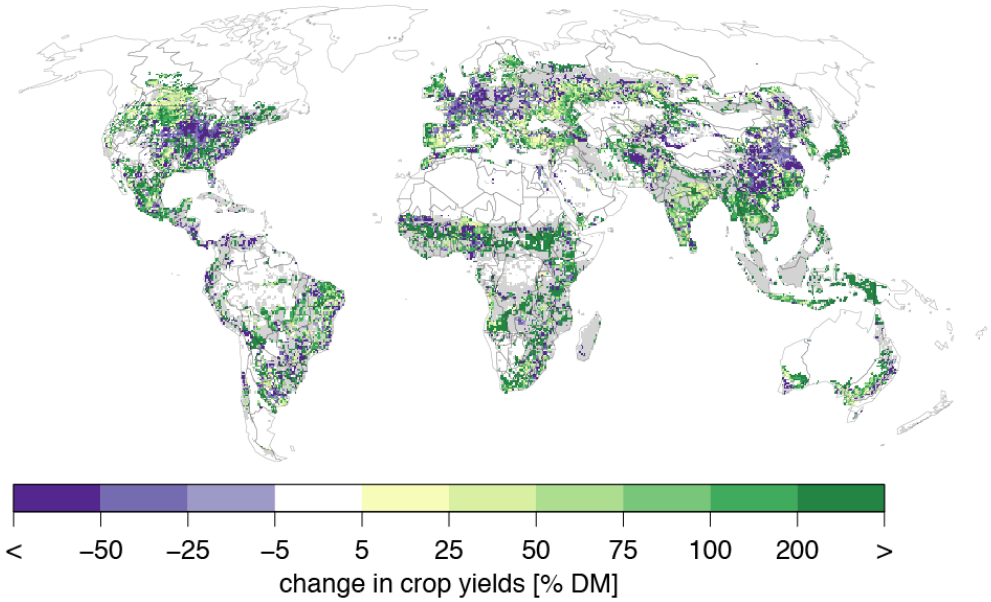

Supplementary Figure 11. Simulated changes in crop yields (end-scenario *vs.* baseline). Differences in area-weighted average yields of 12 major crop types (dry matter, in %), calculated as the difference between the yields underlying the sustainable intensification scenario (areal expansion and improved management, corresponding to Fig. 3f) and the baseline, divided by the latter. Negative values indicate that yield losses due to boundary restrictions dominate, positive values indicate dominance of yield gains due to opportunities (compare Suppl. Fig. 4 for identification of underlying patterns). Grey areas indicate absence of cropland either in the baseline or the sustainable intensification scenario. The simulated global average yield increase is 27%, from 2.82 t ha^{-1} in the baseline to 3.58 t ha^{-1} in this scenario.

Supplementary Tables

Supplementary Table 1. Evaluation of global estimates of simulated key variables against independent datasets.

Variable	LPJmL simulation [reference period]	Range other estimates [reference period]
Total production (incl. losses for animal feed and food waste)*	9.16 * 10^{15} kcal [2005]	9.5 * 10^{15} kcal [2006][6,7]
Vegetal production (excl. post-production losses)*	4.91 * 10^{15} kcal [2005]	5.34 *10^{15} kcal [2005][8]
Irrigation water use	2,498 km^3 yr^{-1} [1980–2009]	2,217–3,185 km^3 yr^{-1}, range *cf.* different studies [various recent periods][9]
Irrigation water consumption	1,275 km^3 yr^{-1} [1980–2009]	927–1,530 km^3 yr^{-1}, range *cf.* different studies [various recent periods][9]
N (reactive) in harvested crops	61 Mt Nr [2005]	72, 74 Mt Nr [2005, 2010][4,10]
N leaching and runoff from natural / agricultural land (and parts thereof reaching surface waters)	34 (24) / 42 (30) Mt Nr [2005]	35[11**] (22)[12***] / 39[13] (33)[12] Mt Nr [2000]
Soil carbon stock****	1,869 PgC [2009–2011]	2,352 ± 400 PgC [2009–2011][14]
Vegetation carbon stock	507 PgC [2009–2011]	445 ± 8 PgC [2009–2011][14]
Gross primary production	124 PgC yr^{-1} [1982–2011]	123 ± 8 PgC^{-1} [1982–2005][15]; 119 ± 6 PgC^{-1} [1982–2005][16]
Net primary production	57 PgC^{-1} [1982–2011]	54 ± 10 PgC^{-1} [1982–2011][14]
Biomass burning through fires	2.7–2.8 PgC^{-1} [1996–2005]	2.33 PgC^{-1} [1996–2005][17]

* Slight underestimations due mainly to lack of explicit simulation of multi-cropping systems.

** Estimate for a natural state without human land-use and without anthropogenic increase in atmospheric deposition.

*** Estimate also includes contribution of vegetation in floodplains.

**** Values in this and the following rows taken from a comprehensive evaluation[18] (using a slightly different LPJmL version) that provides more details on spatial patterns, causes of possible biases, and evaluations of further processes. Ranges in other estimates stem from different data sources and methods including their respective uncertainties (see references for details).

Supplementary Table 2. Average regional livestock feed requirements and livestock product (LP) dietary energy and protein contents. Roughage productivity: roughage requirement based on LPJmL-computed management-corrected roughage and livestock production from Food Balance Sheets (FBS). Crop feed productivity: total human-edible crop feed requirement based on FBS feed data, aggregated by CFTs (adjusted for LPJmL CFT production) and FBS livestock production. Energy (protein) content: dietary energy (protein) content based on FBS food supply quantities.

Region	Roughage productivity (kg roughage DM / kg LP)	Crop feed productivity (total kg FM / kg LP)	Energy content (kcal / kg LP)	Protein content (g protein / kg LP)
Australia & Oceania	5.38	0.29	707.12	47.55
Central America	2.89	1.08	972.75	66.48
East Asia	1.89	1.59	1903.27	91.03
East Europe & Central Asia	1.89	1.32	764.34	49.49
South Asia	5.72	0.25	641.28	42.99
Latin America	4.55	0.86	1039.26	70.68
Southern Africa	11.16	2.29	1015.92	66.49
Middle East	2.93	0.92	809.37	58.34
North Africa	4.21	0.90	808.78	59.41
North America	1.92	1.53	831.41	63.05
Southeast Asia	13.69	2.53	1971.44	103.73
Western Europe	1.28	1.26	758.60	52.24

Supplementary Table 3. Average regional crop share of the total edible crop feed requirements of the aggregated livestock product (LP). Relative amount (%) of feed (FM; Suppl. Table 2) of each crop type represented in LPJmL used to produce the regional average LP.

	Crop functional type (CFT)												
Region	Wheat	Rice	Maize	Millet	Lentils	Sugar beet	Cassava	Sunflower	Soybean	Ground nuts	Rapeseed	Sugar cane	Others
Australia & Oceania	37.0	0.0	1.7	7.9	11.4	0.0	0.0	0.4	4.4	0.0	2.5	1.3	33.5
Central America	3.5	1.0	42.4	11.0	0.2	0.0	1.7	0.0	16.1	0.1	0.0	9.1	14.9
East Asia	2.8	3.9	34.8	1.3	0.8	0.1	2.3	0.3	11.0	1.3	2.0	0.4	38.9
East Europe & Central Asia	36.5	0.0	19.8	0.6	1.3	5.0	0.0	1.6	1.4	0.0	0.4	0.0	33.5
South Asia	4.4	7.4	9.7	1.0	4.8	0.0	0.2	1.1	3.7	7.6	8.2	17.9	34.0
Latin America	1.0	0.3	47.2	3.5	0.1	0.1	23.6	1.1	11.9	0.2	0.0	5.5	5.4
Southern Africa	0.1	0.5	11.5	5.7	1.6	0.0	55.0	0.5	1.3	2.1	0.0	0.5	21.1
Middle East	51.5	1.6	16.3	0.2	1.2	2.0	0.0	2.5	5.2	0.1	0.0	0.0	19.4
North Africa	28.2	0.8	34.1	14.5	1.7	1.4	0.0	1.7	2.6	2.5	0.1	9.3	3.1
North America	7.1	0.0	69.7	0.9	0.3	0.6	0.0	0.3	14.5	0.1	0.9	0.5	5.1
Southeast Asia	2.0	24.9	26.7	0.4	1.4	0.0	12.7	0.2	13.9	0.7	0.1	7.2	9.8
Western Europe	39.9	0.1	24.4	0.1	1.9	1.1	0.0	2.2	17.8	0.0	2.9	0.0	9.5

Supplementary Discussion

Additional livestock intensification scenario

We analyse a scenario reflecting transformation of the livestock sector toward a more industrialized system combined with all other changes considered in the main analysis. For this, we assume the livestock sector of all world regions to converge toward western European conditions. This is done by halving the gap (relative to those conditions), per world region, regarding the roughage and crop feed productivities, the energy and nutritional contents of the average livestock product (i.e. changing the parameters roughage productivity, crop feed productivity, dietary energy content and protein content, listed in Suppl. Table 2 for the main analysis) – similar to scenarios in ref.[19]. Note that for crop feed productivity, the gap in total human edible crop kcal (not FM) was halved, maintaining the region's relative amount of each crop type.

As globally 9.2 $*10^{15}$ kcal yr^{-1} can be produced under these conditions (slightly more than the 8.8 $*10^{15}$ kcal yr^{-1} without such a transformation *cf.* Table 2), this results in a somewhat higher estimate of the population size potentially supplied with the ADER diet, i.e. 10.7 bn people (range *cf.* lower and upper regional ADER values: 10.1–11.5 bn). Analogously, if the low-demand MDER would apply, 13.7 (13.0–14.4) bn people could be fed. While we thus find that a further intensification of the livestock sector would help to increase food supply within PBs (in line with findings from an independent study[20]), more nuanced options for livestock intensification – and associated feedbacks (e.g. a shift from roughage feed to concentrate feed in many regions, leading to a reduction of pastures, increasing pressure on cropland, thus introducing tradeoffs in water and nutrient cycles) – would induce somewhat weaker or stronger productivity changes and environmental footprints[21–24].

Sensitivity test for N:C ratio

In a further sensitivity analysis, we compared results applying two different C:N ratios on LPJmL-simulated yields. The main analysis is based on values from a newly developed model version (LPJmL5) incorporating the N cycle[25]. If values from another source are applied[4], both the restricting effect of maintaining the PB for N flows and the N-related opportunities are somewhat more pronounced. Applying these different values, a food supply (ADER) sufficient for 10.4 bn people would result, i.e. slightly above the present estimate of 10.2 bn. In future studies this PB will be fully integrated into LPJmL5 (which was not yet achievable in this study due to parallel development of model versions). With such an improved model, interlinked effects of nutrient and water management could be simulated consistently as well – e.g. testing if assuming less ambitious improvements in water management would actually result in lower kcal gains[2] or if co-beneficial effects would predominate.

Nitrogen implications of end-scenario including all opportunities

N_2O emissions stem mainly from nitrification and denitrification processes in cropland and pasture soils (estimated at 3.0 and 2.5 Mt N_2O in 2005, respectively; www.fao.org/faostat, accessed 6 Nov 2019), and from animal waste management systems (0.4 Mt N_2O). According to IPCC guidelines[26], N_2O emissions scale linearly with N inputs such as inorganic fertilizers, manure or crop residues. In the simple method applied here, we do not explicitly estimate which form of N input is applied, thus we cannot apply these guidelines to estimate N_2O emissions. As a rough approximation, however, we scale current N_2O emissions from cropland soils with total N inputs, assuming constant composition of various forms of N in the inputs. For the scenario including all opportunities, this results in a reduction of N_2O emissions from croplands soils from 3.0 (baseline) to 2.1 Mt yr^{-1}. Scaling emissions with the N inputs as suggested by IPCC may however overestimate emissions if N use efficiency is strongly improved, as emissions can only stem from the surplus N not incorporated in plant biomass. When scaling cropland soil emissions with the N surplus instead of the N inputs, these emissions are reduced to just 0.9 Mt N_2O yr^{-1}.

We approximated the emission reductions from enteric fermentation, animal waste management systems and manure excreted on pastures by scaling the emissions from 2005 with the estimated change of animal

calorie production. In the scenario applied in this study, animal calorie demand decreases by 12% relative to the baseline, as a net effect of higher population and lower per capita consumption due to assumed changes in diets and reduced losses. Our estimate does not take into account that improved livestock feeding, animal housing and animal waste management could further strongly reduce non-CO_2 greenhouse gas emissions[27], but rather assumes constant emission intensity of livestock production.

In total, N_2O emissions drop from the current 5.9 to 3.5 Mt N_2O yr^{-1} under the assumption that N_2O scales with N surplus. CH_4 emissions from enteric fermentation and animal waste management drop from 101 to 88 Mt CH_4 yr^{-1}. Note that this is not additive to the C sequestration estimate (see Suppl. Methods) due to different time periods and setups used for the calculation.

Supplementary Methods

Planetary boundary for climate change – carbon (C) balance and climate change effects

To determine the changes in C pools and fluxes associated with our opportunities scenario and their contribution to C sequestration, we compare two simulations performed with LPJmL starting from a 300-yr spin-up (recycling the 1860–1900 climate) that brings soil and vegetation C pools into equilibrium for the respective land-use base (see below for details on climate and land-use input): (i) a reference run based on observed climate for 1950–2009 with land-use patterns held constant at year 2005; (ii) a corresponding scenario run for which we fixed the land-use pattern resulting after considering all opportunities (*cf.* Fig. 3h). The resulting 1980–2009 average size of the total global (vegetation + soil) pools is 1,833 (590 + 1,243) GtC in the reference run and 1,908 (622 + 1,286) GtC in the scenario run, respectively – see Suppl. Fig. 7 for the underlying spatial patterns, demonstrating sequestration potentials mainly in regions where afforestation is simulated (compare Suppl. Fig. 4a). Thus, our maximum opportunities scenario (*cf.* Fig. 3h) corresponds to a sequestration potential of 75 GtC (incl. 32 GtC from regrowth of vegetation) in the absence of climate change impacts during any assumed implementation period in equilibrium. This would possibly offset 42% of the cumulative C release from the land-use change emissions over 1750–2011 (estimated to be 180±80 GtC[28]). Conversely, it implies a 38% expansion of the remaining C budget to achieve the 2°C global warming goal with medium probability (196 GtC cumulatively over 2018–2100[29]). Moreover, the inferred sequestration amount translates to a reduction of atmospheric CO_2 content by ~35 ppm – two third the difference between 403 ppm in 2016[30] and the PB value of 350 ppm, and more than the historical share of land-use emissions of the total release from fossil fuel and land-use emissions (32% out of 555 GtC since 1750[28]). Note that this calculation neglects follow-up effects such as of possible forest management and of energy inputs (for infrastructure, processing, transportation) associated with the simulated land-use changes.

Besides, implementation of the above measures would also strongly reduce non-CO_2 greenhouse gas emissions (see Suppl. Discussion).

It is not the scope of this study to assess effects of further transgression of the PB for climate change (or any other PB). Yet, to illustrate some impacts if global warming reached 1.5–2°C following RCP2.6, Suppl. Fig. 9 shows variants of Fig. 3 based on three climate models[31]. This stand-alone analysis demonstrates that simulated agronomic management opportunities are not critically affected at global level and even benefit from higher CO_2 concentration in some regions.

Calculation of food supply for each opportunities scenario

An overview of calculations regarding kcal food supply (computed from LPJmL-simulated crop and pasture production for each step of the U-turn), the livestock sector and diet change is given in Suppl. Fig. 10.

First, the production data provided at 0.5° spatial resolution were aggregated to FPU scale, later merged with further input data available at country, region or global scale (as described below and illustrated in Suppl. Fig. 10). Specifically, production is simulated for 14 crop functional types (CFTs). Of these, 12 are edible crops, one is grass used as roughage (CFT 14), and one can be split into edible crops and roughage (CFT 13, including

cultivation types not specifically parameterised in the model such as citrus, coffee). The latter share is assumed to be 27.4% globally, being the harvested area share of fodder grasses on areas occupied by types included in that CFT according to the MIRCA2000 dataset[32]. Amounts of edible crops were converted to fresh matter used in both food and feed calculations, while roughages were kept in terms of dry matter. Crop production losses are considered in LPJmL model calibration, which is based on FAOSTAT harvest data after production losses (see below section). We estimate the production losses at country scale as in ref.[33], to be able to reduce those in the food loss reduction scenario. From total edible crop production, we subtract CFT-specific crop feed requirements (more detail below), other uses such as seeds based on FAOSTAT Food Balance Sheets (FBS; www.fao.org/faostat), post-harvest losses, processing losses and food waste using country level percentages based on refs.[33–35]. The resulting net crop food supply (fresh matter) is multiplied with regional factors for the dietary energy and protein content of crops (derived from FBS food supply quantities in terms of energy, protein and mass units) to calculate net kcal and protein supply. The same procedure to estimate net kcal and protein supply is done at the end of the livestock calculations.

Within each of the 12 world regions (listed in Suppl. Fig. 8), the current regional production ratios of different livestock products are preserved by averaging the livestock sector. By aggregating all livestock calories, we avoid complexity connected to co-products such as milk and beef, or the attribution of feed to individual animal types. This provides regional-specific feed baskets and allows scaling livestock production (LP) while ensuring consistent feed composition for different animal species and nutritional contents of LP. For each scenario, LP is based on LPJmL-calculated pasture production scaled with regional factors to represent observed grazing data per GLOBIOM region[36], thus accounting for pasture management practices not directly modelled. Pasture production is subsequently added to roughage production. Roughage requirements per unit of LP were calculated based on the management-adjusted roughage production from LPJmL and regionally aggregated total LP from the FBS. Multiplication of the scenarios' roughage production and the roughage requirement yields the scenario's LP at FPU level, implicitly assuming trade within these. Similar to the roughage requirement, crop feed requirements per unit of LP are calculated based on feed per crop from FBS, aggregated by CFTs and adjusted for LPJmL production amounts. For each scenario, CFT-specific crop feed requirements associated with the scenario's LP are calculated and removed from the edible crops (Suppl. Fig. 10). As for edible crops, the production losses were not removed from the LP estimate (in all scenarios where food losses are unchanged), as FBS, which production is based on, accounts for them. From LP, post-production losses, processing losses and food waste were removed using country-level percentages[33–35], resulting in net livestock supply. From this, net livestock kcal and protein supply are calculated by multiplication with regional factors for dietary energy and protein content, derived from the FBS's food supply quantities of energy, protein and mass units.

Population scenarios vs. supply scenarios

In a final analysis step, we compare the food supply achievable within each world region and globally – constrained by the subglobal PBs and boosted by the expansion and management opportunities – with the respective total food requirement considering future population scenarios according to different (Hyde 3.2) SSPs[36]. For this, the original data (in cap km^{-2}) were converted to total populations per world region, then multiplied with the average dietary energy requirements (ADER) per world region tabulated in FAOSTAT (www.fao.org/economic/ess/ess-fs/ess-fadata). For the main analysis, we took the 2017 ADER global average of 2,355 kcal cap^{-1} d^{-1} and derive net food supply from each SSP scenario's crop and pasture production at FPU level. To address related uncertainties we also apply a regional ADER range (2,207 kcal cap^{-1} d^{-1} in East Africa; 2,514 kcal cap^{-1} d^{-1} in developed countries) as well as the Minimum Dietary Energy Requirement vital to prevent undernourishment (MDER; 1,846 kcal cap^{-1} d^{-1}; range 1,759–1,948 kcal cap^{-1} d^{-1}).

Biosphere model and simulation setup

The LPJmL dynamic global vegetation and water balance model simulates terrestrial biogeochemical processes and water fluxes in direct coupling with the establishment, growth and productivity of major natural and (possibly irrigated) agricultural plant types at 0.5° resolution and daily iterations[9,37]. Growth, distribution and productivity of natural vegetation (9 functional types) is driven by climate forcing, while the distribution

and management of agricultural vegetation (CFTs, rainfed or irrigated) is prescribed using historic data or scenario assumptions – such as those imposed here following the different PB restrictions and expansion/management opportunities (see above).

The model has been subjected to comprehensive validation and sensitivity analyses of biogeochemical, hydrological and agricultural process simulations in previous assessments – namely systematic study of parameter uncertainties[38], evaluation and sensitivity analysis of new modules (such as irrigation systems[9]; see overview in ref.[18]), and multidimensional benchmarking in the context of major model overhauls[18,39–42]. In addition, model sensitivities and dynamic responses to varied input parameters were scrutinized and compared to other models, especially regarding vegetation productivity and crop yields[43–48]. For validation of processes key for our analysis see Suppl. Figs. 1, 2 and Suppl. Table 1. For regions where yield variations or magnitudes are still not well captured – e.g. rice in SE Asia or soybean in China and India (Suppl. Fig. 2) – our results are to be interpreted with some caution. Note though, that dynamics of these specific crops cannot be simulated well by any global model and that reported statistics can be biased as well[49]. Overall, the manifold evaluations of LPJmL build confidence in the agronomic and biophysical robustness of here simulated dynamic crop yield changes in response to PB constraints and development opportunities.

All simulations for this study are based on the CRU TS3.10 monthly climatology for temperature and cloudiness[50] combined with GPCC precipitation data[51]. The number of monthly precipitation days was derived from these data with stochastic disaggregation to daily data[52]. The current land-use data are from ref.[53] with modified irrigation patterns from ref.[9]. In all consecutive simulations (after respecting PBs and applying opportunities), the newly generated land-use and irrigation patterns from the respective previous calculation step are fixed. Crop phenology was calculated after ref.[54], but cropping periods of irrigated areas in tropical and precipitation-driven climates were forced to the dry period to better account for the water requirements of multi-cropping systems (rainfed in the humid and irrigated in the dry period). Model simulations from 1950–2009 followed a 900-year spin-up without anthropogenic land-use and a 120-year spin-up based on the scenario's fixed land-use pattern first recycling climate for 1860–1900, then using transient climate for 1901–2009. Crop-specific management was calibrated against national FAO statistics for years 2000–2009. This is done by accordingly varying proxy parameters for management intensity (a crop-specific maximum attainable leaf area index between 1 and 7 m^2 m^2) directly coupled with a maximum harvest index (assuming that high-yielding crop varieties grow on intensively managed fields) and a parameter representing cropping density[53]. Yields change dynamically in our scenarios, e.g. in response to the complex changes in cropping areas and management intensities, as indicated in Suppl. Fig. 11. All obtained results are averaged over the period 1980–2009, as we did not perform transient simulations for a specific future time period.

Supplementary References

[1] GRDC. The Global Runoff Data Centre, 56068 Koblenz, Germany (2016).

[2] J. Jägermeyr, A. Pastor, H. Biemans, D. Gerten, Reconciling irrigated food production with environmental flows for Sustainable Development Goals implementation. *Nat. Commun.* **8**, 15900 (2017).

[3] FAOSTAT. Food and Agricultural Organization of the United Nations (2012).

[4] L. Lassaletta, G. Billen, B. Grizzetti, J. Anglade, J. Garnier, 50 year trends in nitrogen use efficiency of world cropping systems: the relationship between yield and nitrogen input to cropland. *Environ. Res. Lett.* **9**, 105011 (2014).

[5] D. Deryng *et al.*, Regional disparities in the beneficial effects of rising CO_2 concentrations on crop water productivity. *Nat. Clim. Change* **6**, 786–790 (2016).

[6] N. Alexandratos, J. Bruinsma, *World Agriculture Towards 2030/2050: the 2012 Revision.* Technical Report 12 (FAO, 2012).

[7] T. Searchinger *et al.*, *Creating a Sustainable Food Future – a Menu of Solutions to Sustainably Feed More Than 9 Billion People by 2050.* Technical Report (World Resources Institute, 2013).

[8] FAOSTAT, www.fao.org/faostat/en/#data/FBS (last access 28 May 2019).

[9] J. Jägermeyr *et al.*, Water savings potentials of irrigation systems: dynamic global simulation. *Hydrol. Earth Syst. Sci.* **19**, 3073–3091 (2015).

[10] X. Zhang *et al.*, Managing nitrogen for sustainable development. *Nature* **528**, 51–59 (2015).

[11] P. M. Vitousek, D. N. L. Menge, S. C. Reed, C. C. Cleveland, Biological nitrogen fixation: rates, patterns and ecological controls in terrestrial ecosystems. *Phil. Trans. Royal Soc. B* **368**, 1–9 (2013).

[12] A. H. W. Beusen *et al.*, Coupling global models for hydrology and nutrient loading to simulate nitrogen and phosphorus retention in surface water – description of IMAGE–GNM and analysis of performance. *Geosci. Model Dev.* **8**, 4045–4067 (2015).

[13] A. F. Bouwman *et al.*, Exploring global changes in nitrogen and phosphorus cycles in agriculture induced by livestock production over the 1900–2050 period. *Proc. Natl. Acad. Sci.* **110**, 20882–20887 (2011).

[14] N. Carvalhais *et al.*, Global covariation of carbon turnover times with climate in terrestrial ecosystems. *Nature* **514**, 213–217 (2014).

[15] C. Beer *et al.*, Terrestrial gross carbon dioxide uptake: global distribution and covariation with climate. *Science* **329**, 834–838 (2010).

[16] M. Jung *et al.*, Global patterns of land-atmosphere fluxes of carbon dioxide, latent heat, and sensible heat derived from eddy covariance, satellite, and meteorological observations. *J. Geophys. Res. – Biogeo.* **116**, G00J07 (2011).

[17] J. Randerson *et al.*, *Global Fire Emissions Database*, Version 4, (GFEDv4), ORNL DAAC, doi.org/10.3334/ORNLDAAC/1293 (2015).

[18] S. Schaphoff *et al.*, LPJmL4 – a dynamic global vegetation model with managed land: part 2 – model evaluation. *Geosci. Model Dev.* **11**, 1377–1403 (2018).

[19] B. L. Bodirsky *et al.*, N_2O Emissions from the global agricultural nitrogen cycle – current state and future scenarios. *Biogeosci.* **9**, 4169–4197 (2012).

[20] M. Springmann *et al.*, Options for keeping the food system within environmental limits. *Nature* **562**, 519–525 (2018).

[21] I. Weindl *et al.*, Livestock production and the water challenge of future food supply: implications of agricultural management and dietary choices. *Global Environ. Change* **47** (Suppl. C), 121–32 (2017).

[22] I. Weindl *et al.* Livestock and human use of land: productivity trends and dietary choices as drivers of future land and carbon dynamics. *Global Planet. Change* **159** (Suppl. C), 1–10 (2017).

[23] B. L. Bodirsky *et al.*, N_2O emissions of the global agricultural nitrogen cycle – current state and future scenarios. *Biogeosci.* **9**, 4169–4197 (2012).

[24] M. Herrero *et al.*, Biomass use, production, feed efficiencies, and greenhouse gas emissions from global livestock systems. *Proc. Natl. Acad. Sci. USA* **110**, 20888–20893 (2013).

[25] W. von Bloh *et al.*, Implementing the nitrogen cycle into the dynamic global vegetation, hydrology, and crop growth model LPJmL (version 5.0). *Geosci. Model Dev.* **11**, 2789–2812 (2018).

[26] IPCC, *2006 IPCC Guidelines for National Greenhouse Gas Inventories, Prepared by the National Greenhouse Gas Inventories Programme*, H. S. Eggleston *et al.*, Eds. (IGES, 2006).

[27] R. H. Beach *et al.*, Global mitigation potential and costs of reducing agricultural non-CO_2 greenhouse gas emissions through 2030. *J. Integr. Env. Sci.* **12** (Suppl. 1), 87–105 (2015).

[28] P. Ciais *et al.*, "Carbon and other biogeochemical cycles" in *Climate Change 2013: The Physical Science Basis. Contribution of Working Group I to the Fifth Assessment Report of the Intergovernmental Panel on Climate Change*, T. F. Stocker *et al.*, Eds. (Cambridge University Press, Cambridge & New York, 2013).

[29] IPCC, "Summary for Policymakers" in *Climate Change 2014: Mitigation of Climate Change. Contribution of Working Group III to the Fifth Assessment Report of the Intergovernmental Panel on Climate Change*, O. Edenhofer *et al.*, Eds. (Cambridge University Press, Cambridge & New York, 2014).

[30] C. Le Quéré *et al.*, Global carbon budget 2017. *Earth Syst. Sci. Data* **10**, 405–448 (2018).

[31] S. Ostberg, L. Boysen, S. Schaphoff, D. Gerten, The biosphere under potential Paris outcomes. *Earth's Fut.* **6**, 23–39 (2018).

[32] F. T. Portmann, S. Siebert, P. Döll, MIRCA2000 – global monthly irrigated and rainfed crop areas around the year 2000: a new high-resolution data set for agricultural and hydrological modeling. *Global Biogeochem. Cy.* **24**, GB1011 (2010).

[33] M. Jalava *et al.*, Diet change and food loss reduction: what is their combined impact on global water use and scarcity? *Earth's Fut.* **4**, 62–78 (2016).

[34] M. Kummu *et al.*, Bringing it all together: linking measures to secure nations' food supply. *Curr. Op. Environ. Sust.* **29**, 98–117 (2017).

[35] J. Gustavsson *et al.*, *Global Food Losses and Food Waste: Extent, Causes and Prevention* (FAO, 2011).

[36] C. G. M. Klein Goldewijk (Utrecht University), *A historical land use data set for the Holocene; HYDE 3.2 (replaced).*

DANS. https://doi.org/10.17026/dans-znk-cfy3 (2016).

[37] S. Schaphoff *et al.*, Contribution of permafrost soils to the global carbon budget. *Environ. Res. Lett.* **8**, 014026 (2013).

[38] S. Zaehle, S. Sitch, B. Smith, F. Hattermann, Effects of parameter uncertainties on the modeling of terrestrial biosphere dynamics. *Global Biogeochem. Cycl.* **19**, GB3020 (2005).

[39] S. Sitch *et al.*, Evaluation of ecosystem dynamics, plant geography and terrestrial carbon cycling in the LPJ dynamic global vegetation model. *Glob. Chang. Biol.* **9**, 161–185 (2003).

[40] A. Bondeau *et al.*, Modelling the role of agriculture for the 20th century global terrestrial carbon balance. *Global Change Biol.* **13**, 679–706 (2007).

[41] S. Rost *et al.*, Agricultural green and blue water consumption and its influence on the global water system. *Water Resour. Res.* **44**, W09405 (2008).

[42] C. Müller *et al.*, Global gridded crop model evaluation: benchmarking, skills, deficiencies and implications. *Geosci. Model Dev.* **10**, 1403–1422 (2017).

[43] D. Gerten *et al.*, Modelled effects of precipitation on ecosystem carbon and water dynamics in different climatic zones. *Global Change Biol.* **14**, 2365–2379 (2008).

[44] S. Asseng *et al.*, Uncertainty in simulating wheat yields under climate change. *Nat. Clim. Change* **3**, 827–832 (2013).

[45] C. Müller *et al.*, Implications of climate mitigation for future agricultural production. *Environ. Res. Lett.* **10**, 125004 (2015).

[46] N. Pirttioja *et al.*, Temperature and precipitation effects on wheat yield across a European transect: a crop model ensemble analysis using impact response surfaces. *Clim. Res.* **65**, 87–105 (2015).

[47] B. Schauberger *et al.*, Consistent negative response of US crops to high temperatures in observations and crop models. *Nat. Commun.* **8**, 13931 (2017).

[48] C. F. Schleussner *et al.*, Crop productivity changes in 1.5° C and 2° C worlds under climate sensitivity uncertainty. *Environ. Res. Lett.* **13**, 064007 (2018).

[49] M. Heino *et al.*, Two-thirds of global food production impacted by climate oscillations. *Nat. Commun.* **9**, 1257 (2018).

[50] I. Harris, P. D. Jones, T. J. Osborn, D. H. Lister, Updated high-resolution grids of monthly climatic observations – the CRU TS3.10 dataset. *Int. J. Climatol.* **34**, 623–642 (2014).

[51] U. Schneider *et al.*, GPCC's new land surface precipitation climatology based on quality-controlled in situ data and its role in quantifying the global water cycle. *Theor. Appl. Climatol.* **115**, 15–40 (2014).

[52] J. Heinke *et al.*, A new climate dataset for systematic assessments of climate change impacts as a function of global warming. *Geosci. Mod. Dev.* **6**, 1689–1703 (2013).

[53] M. Fader, S. Rost, C. Müller, A. Bondeau, D. Gerten, Virtual water content of temperate cereals and maize: present and potential future patterns. *J. Hydrol.* **384**, 218–231 (2010).

[54] K. Waha, L. G. J. van Bussel, C. Müller, A. Bondeau, Climate-driven simulation of global crop sowing dates. *Global Ecol. Biogeogr.* **21**, 247–259 (2012).